

Electronic structure studies of diradicals derived from *Closo*-Carboranes

Josep M. Oliva · Diego R. Alcoba · Luis Lain · Alicia Torre

Received: 27 September 2012 / Accepted: 29 December 2012
© Springer-Verlag Berlin Heidelberg 2013

Abstract Electronic structure computations have been performed on diradical systems composed of two carborane radicals $\text{CB}_{11}\text{H}_{12}^{\cdot}$ connected through acetylene, ethylene and ethane bridge units, leading, respectively, to a *linear* and two *trans* structures. Each cage possesses one unpaired electron and the total system can thus be coupled to a singlet or a triplet state. Numerical determinations using the spin-projected method with a hybrid B3LYP functional show that these compounds have singlet ground states with low singlet–triplet energy gaps of 0.004 eV (acetylene bridge), 0.080 eV (ethylene bridge) and 0.0005 eV (ethane bridge). Spin population analyses point out a left/right localized spin distribution in the spin-projected wave function. The possibility of mapping these results onto a Heisenberg spin Hamiltonian is considered, in order to

predict low-lying excited states in extended carborane chains.

Keywords Carboranes · Spin population · Heisenberg spin Hamiltonian · Heisenberg coupling constants

1 Introduction

Polyhedral boron chemistry embraces fields of research in inorganic chemistry at both molecular and solid-state levels and, in combination with organic moieties and metals [1], provides applications of interest in material sciences [2], design of pharmacophores [3] and medicine [4]. Thus, a wide variety of molecular and solid-state architectures have been synthesized since the first days of the synthesis of the *closo*-borane cages, particularly with the well-known icosahedral *closo*-borane anion $\text{B}_{12}\text{H}_{12}^{2-}$ [5]. One of the most challenging aspects of polyhedral boron chemistry is the study of low-lying excited states, as opposed to the (more) well-known excited state chemistry of carbon-derived compounds in organic chemistry—see for instance references [6, 7]. When boron cage atoms are substituted by carbon atoms in the icosahedral $\text{B}_{12}\text{H}_{12}^{2-}$ dianion, one then obtains the clusters from the series $\text{C}_n\text{B}_{12-n}\text{H}_{12}^{(n-2)}$, the so-called carboranes [8]. In the last few years, we have been interested in the electronic structure of ground states and excited states derived from polyhedral borane and carborane molecules, as *isolated* units [9–11], or connected in linear [12, 13] and triangular configurations [14, 15]. The versatile combination of charge and spin in these systems offers the possibility of tuning the properties of molecular architectures based on heteroborane cage units.

The $\text{CB}_{11}(\text{CH}_3)_{12}^{\cdot}$ radical [16]—with one unpaired electron—can be connected in 1D, 2D and 3D architectural

Published as part of the special collection of articles derived from the 8th Congress on Electronic Structure: Principles and Applications (ESPA 2012).

J. M. Oliva (✉)
Instituto de Química-Física “Rocasolano”, Consejo Superior de Investigaciones Científicas, 28006 Madrid, Spain
e-mail: j.m.oliva@iqfr.csic.es

D. R. Alcoba
Departamento de Física, Facultad de Ciencias Exactas y Naturales, Universidad de Buenos Aires, Ciudad Universitaria, 1428 Buenos Aires, Argentina

D. R. Alcoba
Instituto de Física de Buenos Aires, Consejo Nacional de Investigaciones Científicas y Técnicas, Ciudad Universitaria, 1428 Buenos Aires, Argentina

L. Lain · A. Torre
Departamento de Química Física. Facultad de Ciencia y Tecnología, Universidad del País Vasco,
Apdo. 644, 48080 Bilbao, Spain

constructions thus involving a polyradical system with a determined number of unpaired electrons. So far to our knowledge, only the diradicals $[(\text{CH}_3\text{B})_{11}\text{C}-\text{C}\equiv\text{C}-\text{C}(\text{BCH}_3)_{11}]^\cdot$ and *trans*- $[(\text{CH}_3\text{B})_{11}\text{C}-\text{CH}=\text{CH}-\text{C}(\text{BCH}_3)_{11}]^\cdot$ have been synthesized [17]. Recently, we have studied the electronic structure of the simplified diradical $[(\text{HB})_{11}\text{C}-\text{C}\equiv\text{C}-\text{C}(\text{BH})_{11}]^\cdot$ [12] using high-level quantum chemical models—CASPT2 [18]—for the calibration of the spin-projected method with the hybrid functional UB3LYP. These studies have shown that the ground state in the diradical is of singlet state nature, having a low-lying triplet state 0.005 eV (CASPT2) higher in energy ($k_B T$ at room temperature is 0.025 eV/0.6 kcal/mol). This energy difference corresponds to the microwave region of the electromagnetic spectrum and therefore one could in principle populate selectively the triplet state using microwave photons, provided that intersystem crossing and spin-orbit interactions are significant. This energy difference also corresponds to rotational modes in gas-phase molecules, molecular motions in liquids and phonons in solids [19].

Let us now consider two icosahedral *closo*-carborane $\text{CB}_{11}\text{H}_{12}$ radicals, each of them with one unpaired electron ($S = 1/2$), that might be connected in *para* position through the carbon atom of the cage with an acetylene, ethylene or ethane bridge unit. The three resulting structures are depicted in Fig. 1.

We will proceed to study the electronic structure of these compounds applying spin-partitioning techniques: Which are the (estimated) singlet–triplet energy gaps—or the corresponding spin–spin coupling constants, J 's—in these diradicals? How are the electronic structures of the triplet states as compared to the spin-projected symmetry states? These are the questions we would like to answer in this work.

2 Methodology

All computations in this work have been carried out at the (U)B3LYP/6-31 + G(d) level of theory with the suite of programs Gaussian [20]. Geometry optimizations have been performed for the triplet states and spin-projected states, corresponding all structures to energy minima. The spin-projected method for two electrons was developed in Ref. [21], which reports a spin-unrestricted wave function, $\Psi_{\text{unr},S}$, with both singlet and triplet components:

$$\Psi_{\text{unr},S} = a \cdot \Psi_S + b \cdot \Psi_T; \quad a^2 + b^2 = 1. \quad (1)$$

The wave functions Ψ_S and Ψ_T are “pure” spin states with $S = 0$ (singlet) and $S = 1$ (triplet), respectively. One can then show that

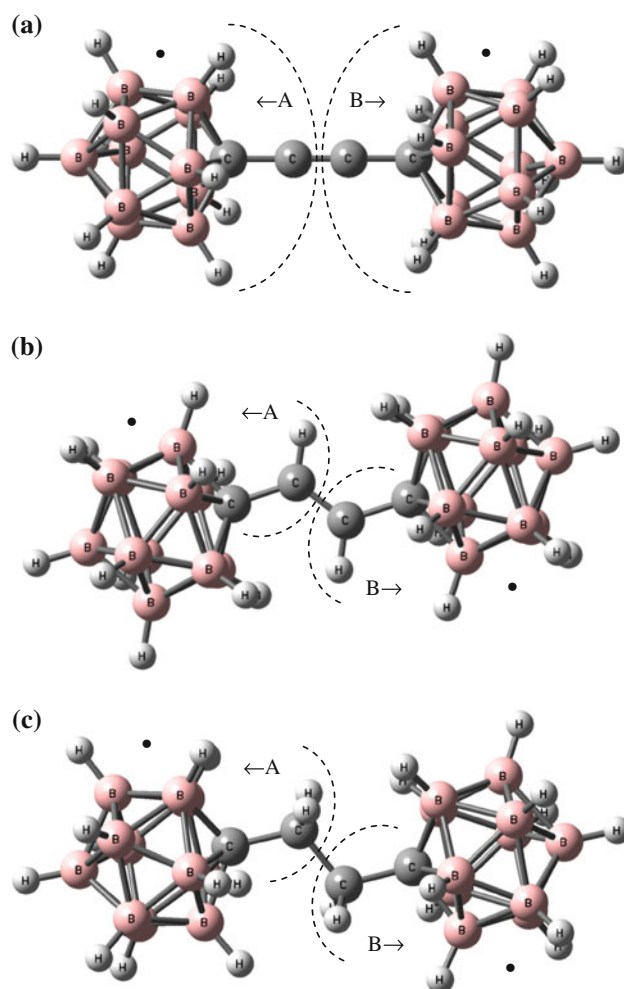


Fig. 1 The three diradicals described in this work: Two *closo*-carborane radicals $\text{CB}_{11}\text{H}_{12}^\cdot$ connected through the cage carbon atom with **a** an acetylene bridge unit, **b** an ethylene bridge unit and **c** an ethane bridge unit. The *dots* represent unpaired electrons. The *dashed curves* divide the molecule into two fragments, denoted as *A* and *B*

$$b^2 = \frac{1}{2} \langle \Psi_{\text{unr},S} | \hat{S}^2 | \Psi_{\text{unr},S} \rangle \quad (2)$$

and therefore the singlet–triplet energy gap— ΔE_{ST} —can be estimated as:

$$\Delta E_{\text{ST}} = (E_{\text{unr},S} - E_T) / (1 - b^2) \quad (3)$$

On the other hand, the phenomenological Heisenberg spin Hamiltonian—Eq. 4—predicts the energy of the different spin states of a many-electron system, provided the spin degrees of freedom are independent from the electron (orbital) degrees of freedom

$$\hat{H} = -2 \sum_{A > B} J_{AB} \hat{S}_A \cdot \hat{S}_B \quad (4)$$

where \hat{S}_A and \hat{S}_B are the local spin operators associated with the neighbor molecular units *A* and *B*, respectively, which may be atoms or molecular fragments. J_{AB} are the

corresponding Heisenberg coupling constants, which may be related directly to a singlet–triplet energy difference for a two-electron system. Thus, the eigenspectrum of \hat{H} connects experimental and theoretical studies of magnetism in molecular systems.

If we divide a cluster, molecule, etc., into different fragments A, B, ..., the information on the spin attributed to these fragments may be obtained from the expectation values of the local spin operators $\langle \hat{\mathbf{S}}_A^2 \rangle$ and $\hat{\mathbf{S}}_A \cdot \hat{\mathbf{S}}_B$ [22, 23]

$$\langle \hat{\mathbf{S}}^2 \rangle = \sum_A \sum_B \langle \hat{\mathbf{S}}_A \cdot \hat{\mathbf{S}}_B \rangle \quad (5)$$

The one-center local spin $\langle \hat{\mathbf{S}}_A^2 \rangle$ allows one to determine the spin state of an atom or group of atoms in a molecule or cluster, while the spin correlation between fragments A and B is described by the expectation value $\langle \hat{\mathbf{S}}_A \cdot \hat{\mathbf{S}}_B \rangle$. This value provides an important tool for linking experimental results interpreted in terms of the Heisenberg spin Hamiltonian to quantum chemical calculations, as mentioned above. We will consider the general algebraic expression for $\langle \hat{\mathbf{S}}_A \cdot \hat{\mathbf{S}}_B \rangle$ reported in Refs. [24, 25], which for the case of a Slater determinant wave function has the form

$$\langle \hat{\mathbf{S}}_A \cdot \hat{\mathbf{S}}_B \rangle = \frac{1}{4} \sum_{\mu \in A} \sum_{\nu \in B} (\mathbf{P}^s \mathbf{S})_{\mu\mu} \cdot (\mathbf{P}^s \mathbf{S})_{\nu\nu} + \delta_{AB} \frac{1}{2} \sum_{\mu \in A} \sum_{\nu \in B} (\mathbf{P}^s \mathbf{S})_{\mu\nu} \cdot (\mathbf{P}^s \mathbf{S})_{\nu\mu} \quad (6)$$

where μ, ν, \dots are the atomic functions used, $\mathbf{P}^s = \mathbf{P}^\alpha - \mathbf{P}^\beta$ the spin density matrix and \mathbf{S} the overlap matrix. In this equation, the sums are restricted to the atomic orbitals assigned to the corresponding fragment.

Several procedures have been proposed for the calculation of the coupling constants J_{AB} . In the Yamaguchi approach (YA) [26], these constants can be calculated as the energy difference between the high-spin ferromagnetic state (hs) and the spin-projected antiferromagnetic state (sp) determinants divided by the difference of their respective $\hat{\mathbf{S}}^2$ operator expectation values, that is

$$J_{AB}(\text{YA}) = - \frac{{}^{\text{hs}}E - {}^{\text{sp}}E}{\langle \hat{\mathbf{S}}^2 \rangle_{\text{hs}} - \langle \hat{\mathbf{S}}^2 \rangle_{\text{sp}}} \quad (7)$$

Alternatively, in the local spin approach (LS), the coupling constants can also be calculated by means of the energy difference between the high-spin ferromagnetic state (hs) and the spin-projected antiferromagnetic state (sp) determinants divided by twice the difference of the two-center local spins in the form [27]

$$J_{AB}(\text{LS}) = - \frac{{}^{\text{hs}}E - {}^{\text{sp}}E}{2 \left(\langle \hat{\mathbf{S}}_A \cdot \hat{\mathbf{S}}_B \rangle_{\text{hs}} - \langle \hat{\mathbf{S}}_A \cdot \hat{\mathbf{S}}_B \rangle_{\text{sp}} \right)} \quad (8)$$

3 Results and discussion

The three carborane diradicals which arise from the connection of two radicals $\text{CB}_{11}\text{H}_{12}$ through an acetylene, ethylene and ethane bridge unit are displayed in Fig. 1. While high-level quantum chemical computations are feasible for these dimers in the future, we would like to extend the system with more units to an (in)finite 1D chain and thus obtain the low-lying spin states, through a mapping of the results onto a Heisenberg spin Hamiltonian. A similar mapping has been carried out for many-electron systems using accurate post-HF calculations onto a generalized spin-exchange Hamiltonian, in clusters of hydrogen atoms [28].

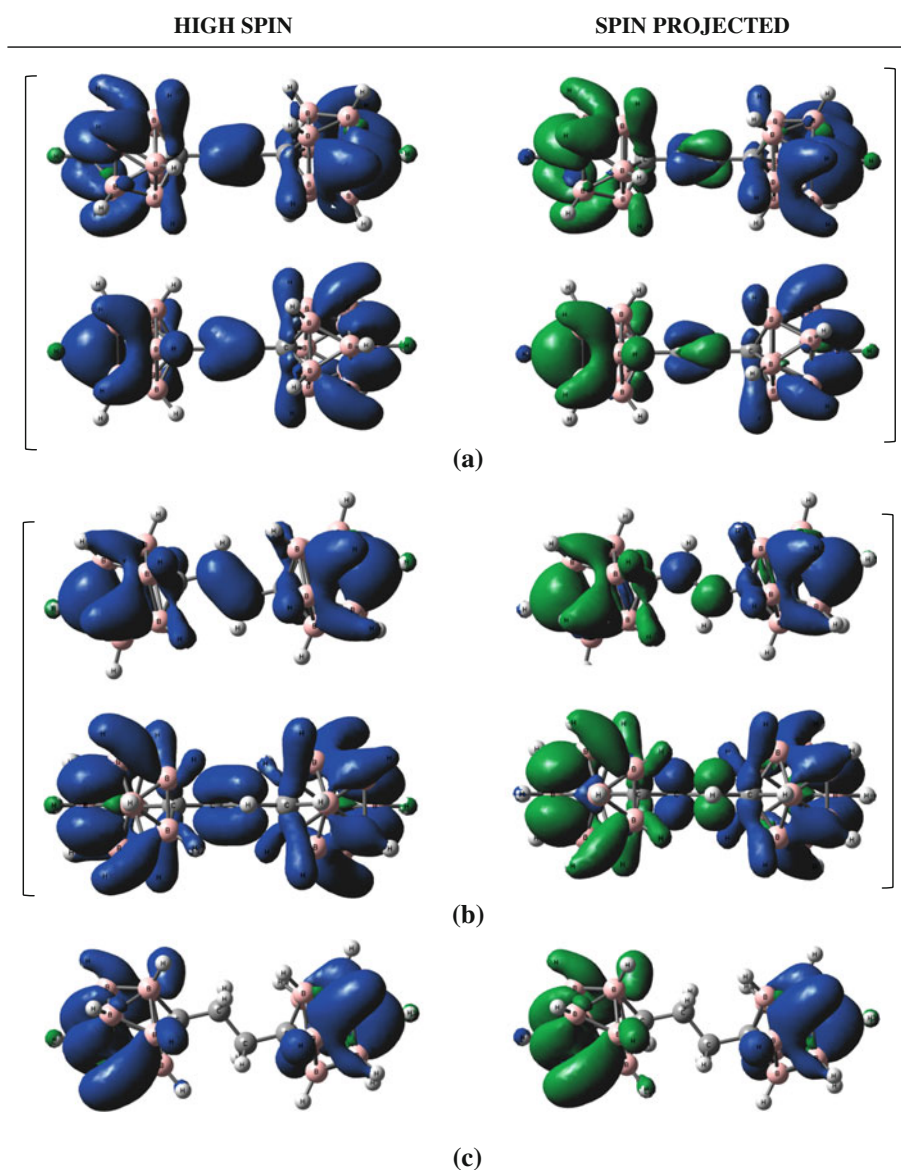
As mentioned in the Introduction, we have obtained the singlet–triplet energy gaps and electronic energies for the structure displayed in Fig. 1a, using the spin-projected method and calibrating the results with very high-level quantum–mechanical computations [12]. The results have shown that the UB3LYP/6-31G(d) spin-projected method compares very well with high-level CASPT2/6-31G(d) computations. For this diradical, the ground state is of singlet nature, with a practically degenerate triplet state only 0.005 eV (CASPT2) higher in energy, which corresponds to the far-IR region of the electromagnetic spectrum, as reported. In this work, the UB3LYP/6-31G(d) spin-projected method has also been applied to the other two structures shown in Fig. 1, in order to know how the unpaired electrons couple to each other in these three structures, that is, when the

Table 1 Local spin populations $\langle \hat{\mathbf{S}}_A \cdot \hat{\mathbf{S}}_B \rangle$ for the diradicals studied in this work; hs and sp stand for high-spin and spin-projected wave function, respectively

Local spins	hs state		sp state	
	A	B	A	B
Acetylene bridge				
A	0.759	0.250	0.662	−0.158
B	0.250	0.749	−0.158	0.662
Ethylene bridge				
A	0.754	0.250	0.488	−0.095
B	0.250	0.753	−0.095	0.485
Ethane bridge				
A	0.752	0.250	0.758	−0.255
B	0.250	0.755	−0.255	0.759

A left moiety, B right moiety—see Fig. 1

Fig. 2 Spin density for the high-spin (triplet) states (*left*) and spin-projected states (*right*) in the three diradicals considered in this work: **a** $(\text{HB})_{11}\text{C}-\text{C}\equiv\text{C}-\text{C}(\text{BH})_{11}$ diradical, **b** $(\text{HB})_{11}\text{C}-\text{CH}=\text{CH}-\text{C}(\text{BH})_{11}$ diradical and **c** $(\text{HB})_{11}\text{C}-\text{CH}_2-\text{CH}_2-\text{C}(\text{BH})_{11}$ diradical. Spin density isovalue $\rho_s = \pm 0.001$ in all plots. For **a** and **b** two orientations of the diradical are considered: the one above corresponds to the same orientation as in Fig. 1. The one below is a 90° rotation of the former around the axis defined by the carbon atoms of the carborane cage



bridge unit connecting the carborane cages is of the acetylene, ethylene and ethane type.

The local spin populations $\langle \hat{\mathbf{S}}_A \cdot \hat{\mathbf{S}}_B \rangle$ (Eq. 6) in the studied diradicals are shown in Table 1, where A and B correspond, respectively, to the left and right moieties, as displayed in Fig. 1. The basis set dependence of atomic spin populations has been recently studied in Ref. [29].

The values found for $\langle \hat{\mathbf{S}}_A^2 \rangle$ quantities in the three studied systems indicate that the hs state presents one-center local spin components close to 0.75 (the canonical value is $\frac{1}{2}(\frac{1}{2} + 1)$), showing that those states possess a spin distribution corresponding to two well-localized electrons, each one in a moiety. The two-center local spin components $\langle \hat{\mathbf{S}}_A \cdot \hat{\mathbf{S}}_B \rangle$ are positive according to the coupling of two electrons to a triplet state and their values are close

to $\frac{1}{4}$. A slight spin contamination is only observed in the one-center terms. The sp states present values of one-center and two-center local spin quite different in the three systems. In the ethane bridge compound the one-center local spin value 0.76 is very close to the canonical one 0.75, meaning that the spin distribution is again that of two well-localized electrons, one in each fragment. However, in the acetylene bridge system the one-center terms have a larger difference respect of the canonical value, which must be interpreted in terms of two unpaired electrons slightly delocalized. This behavior, with a higher deviation from the corresponding canonical value, is also found in the case of the ethylene bridge diradical where the unpaired electrons are still more delocalized. Contrarily to the case of the hs states, the two-center components of the local spins are negative which corresponds to two unpaired electrons

Table 2 Energies (au), expectation values $\langle \hat{S}^2 \rangle$, singlet–triplet gaps ΔE_{ST} (in eV)—Eq. (3)—and coupling constants J_{AB} (in cm^{-1}) for the diradicals studied in this work; hs and sp stand for high-spin ($S = 1$) and spin-projected, respectively

	Energy	$\langle \hat{S}^2 \rangle$	ΔE_{ST}	$J_{AB}(YA)$	$J_{AB}(LS)$
Acetylene bridge					
hs state	-712.56328	2.0075	–	-15.27	-18.71
sp state	-712.56335	1.0079	-0.004		
Ethylene bridge					
hs state	-713.81780	2.0068	–	-321.6	-571.1
sp state	-713.81960	0.7834	-0.080		
Ethane bridge					
hs state	-715.04007	2.0077	–	-1.826	-1.810
sp state	-715.04008	1.0076	-0.0005		

YA and LS stand for Yamaguchi [26] and local spin [27] approaches, respectively

coupled to a singlet state. The values found are close to -0.25 only in the ethane bridge, due to the localization of the electrons in that system.

In order to visualize the spin distribution in these diradicals, Fig. 2 displays the spin density for the high-spin (left) and spin-projected (right) states of the three diradicals, following the same orientations as in Fig. 1. As evident from this Figure, there is clearly a left–right distribution of positive and negative spin density in the spin-projected states corresponding, respectively, to the A and B fragments of each diradical. In the acetylene and ethylene bridge diradicals (Fig. 2a, b), two projections of the spin density are represented—with a rotation of 90° degrees of the top respect to the bottom one, with the rotation around the axis joining the two carbon atoms of the carborane cage—since there is a noticeable contribution from the bridge units to the total spin density, and a different orientation of the molecule is needed in order to highlight the topological differences of the spin density between the acetylene (Fig. 2a) and ethylene (Fig. 2b) bridge units. One could find a topological similarity between the density of a π/π^* molecular orbital and the modulus of the high-spin/spin-projected spin density of the ethylene moiety in Fig. 2b. However, this is not the case for the acetylene bridge diradical, where no nodal planes, but rather nodal surfaces appear to separate the α - and β -spin densities in the bridge moiety. Given the negligible spin density in the ethane bridge diradical, a unique orientation, coinciding with the one from Fig. 1c is displayed in Fig. 2c.

In Table 2 we display the energies, the expectation values $\langle \hat{S}^2 \rangle$ and the coupling constants J_{AB} computed with

the Yamaguchi and local spin approaches, for the three diradicals considered in this work.

As shown in Table 2, the ground state in all three diradicals always corresponds to the estimated singlet state, although the triplet state lies very close in energy with J 's in the order (in absolute value): $J(\text{ethylene}) \gg J(\text{acetylene}) > J(\text{ethane})$. The ethylene bridge (Fig. 1b) thus provides a “strong” interaction between the unpaired electrons in the isolated carborane cage radicals $\text{CB}_{11}\text{H}_{12}^{\cdot}$, which agrees with the local spin values above described for this compound. In the case of the ethane bridge (Fig. 1c), one can assume one almost isolated unpaired electron on each carborane cage, given the practical degeneracy of singlet and triplet states; the ethane bridge does not provide an “electronic coupling” between the spins of the unpaired electrons from A and B fragments. The case of the acetylene bridge (Fig. 1a), already studied in Ref. [12], is an intermediate case, with a significant coupling between the spins of the electrons in the fragments A and B. The numerical values found for the coupling constants in both procedures (YA and LS) are very similar in the case of the ethane bridged diradical. However, these values present a difference for the acetylene bridge, which becomes even larger in the case of the ethylene one. These results are in agreement with the degree of electron localization in these three compounds. In fact, only under the assumption of unpaired electrons localized on the radical centers in both hs and sp states, one should expect similar results for both models [22].

4 Concluding remarks and perspectives

In this work, we have presented a detailed electronic structure analysis of three diradicals derived from the connection of two icosahedral carborane radicals $\text{CB}_{11}\text{H}_{12}^{\cdot}$ through the cage carbon atom with acetylene, ethylene and ethane bridge units. All diradicals have a singlet ground state with very low-lying triplet states. The ethane bridge diradical is practically degenerate, with an energy gap below 1 meV. The acetylene bridge diradical shows a certain coupling between the carborane units, with an energy gap of 4 meV, and the case of ethylene bridge has a higher electron coupling up to 80 meV. These results in terms of energy are consistent with the conclusions arising from the spin population analysis. The local spin values found correspond to the presence of two well-localized electrons in the hs state of each of these compounds, but the analysis for the sp state points out two electrons well-localized (noninteracting) in the case of the ethane bridge, slightly delocalized in the case of acetylene bridge and more delocalized in the ethylene bridge one. The electron

coupling between the carborane cages is due to the ethylene and acetylene bridge unit as clearly shown through spin density plots.

The next challenge is to predict low-lying states in larger polyradical one-dimensional or cyclic chains through a mapping of the current results onto a Heisenberg spin Hamiltonian for a set of carborane clusters. As mentioned above, similar mappings have been performed, for instance in clusters of hydrogen atoms and using accurate post-HF calculations with a further mapping onto a generalized spin-exchange Hamiltonian [28]. This task is currently being performed in our Laboratories.

Acknowledgments This report has been financially supported by the Projects MICINN CTQ2009-13652, UBACYT 20020100100197 (Universidad de Buenos Aires), PIP No. 11220090100061 (Consejo Nacional de Investigaciones Científicas y Técnicas, República Argentina), GIU09/43 (Universidad del País Vasco) and UFI11/07 (Universidad del País Vasco). We thank the Universidad del País Vasco for allocation of computational resources.

References

1. Bould J, Baše T, Londesborough MGS, Oro LA, Macías R, Kennedy RJD, Kubát P, Fuciman M, Polívka T, Lang K (2011) *Inorg Chem* 50:7511
2. van der Vlugt JI (2010) *Angew Chem Int Ed* 49:252
3. Scholz M, Hey-Hawkins E (2001) *Chem Rev* 111:7035
4. El-Zaria ME, Ban HS, Nakamura H (2010) *Chem Eur J* 16:1543
5. Sivaev IB, Bregadze VI, Sjöberg S (2002) *Collect Czech Chem Commun* 67:679
6. Klessinger M, Michl J (1994) *Excited states and photochemistry of organic molecules*. Wiley-VCH, New York
7. Valeur B (2002) *Molecular fluorescence*. Wiley-VCH, Weinheim
8. Grimes RN (2011) *Carboranes*, 2nd edn. Academic Press, New York
9. Serrano-Andrés L, Klein DJ, Schleyer PVR, Oliva JM (2008) *J Chem Theory Comput* 4:1338
10. Oliva JM, Serrano-Andrés L (2006) *J Comput Chem* 27:524
11. Londesborough MG, Hnyk D, Bould J, Serrano-Andrés L, Saurí V, Oliva JM, Kubát P, Polívka T, Lang K (2012) *Inorg Chem* 51:1471
12. Oliva JM, Serrano-Andrés L, Havlas Z, Michl J (2009) *J Mol Struct (Theochem)* 912:13
13. Oliva JM (2012) *Adv Quantum Chem* 64:105
14. Oliva JM (2011) Cyclic spin architectures built from carborane radicals, XXXIII reunión bienal de la Real Sociedad Española de Física, Santander, Spain, 19–23 Septiembre 2011, p 45
15. Oliva JM (2011) 11th international conference on computational and mathematical methods in science and engineering, CMMSE 2011, Alicante, Spain, 16–20 June 2011, p 78
16. King BT, Noll BC, McKinley AJ, Michl J (1996) *J Am Chem Soc* 118:10902
17. Eriksson L, Vyakaranam K, Ludvík J, Michl J (2007) *J Org Chem* 72:2351
18. Roos BO, Andersson K, Fulscher MP, Malmqvist PA, Serrano-Andrés L, Pierloot K, Merchán M (1996) *Adv Chem Phys* 93:219
19. Atkins PW, de Paula J (2009) *Physical chemistry*, 9th edn. Oxford University Press, Oxford
20. Frisch MJ et al (2004) *Gaussian 03*, revision C.02. Gaussian Inc., Wallingford
21. Ovchinnikov AA, Labanowski JK (1996) *Phys Rev A* 53:3946
22. Clark A, Davidson ER (2001) *J Chem Phys* 115:7382
23. Podewitz M, Herrmann C, Malassa A, Westerhausen R, Reiher M (2008) *Chem Phys Lett* 451:301
24. Alcoba DR, Lain L, Torre A, Bochicchio RC (2009) *Chem Phys Lett* 470:136
25. Alcoba DR, Torre A, Lain L, Bochicchio RC (2011) *J Chem Theory Comput* 7:3560
26. Soda T, Kitagawa Y, Onishi T, Takano Y, Shigeta Y, Nagao H, Yoshioka Y, Yamaguchi K (2000) *Chem Phys Lett* 319:223
27. Herrmann C, Yu L, Reiher M (2006) *J Comput Chem* 27:1223
28. Ciofinia I, Adamo C, Barone V, Berthier G, Rassat A (2005) *Chem Phys* 309:133
29. Philips JJ, Hudspeth MA, Browne PM Jr, Peralta JE (2010) *Chem Phys Lett* 495:146